STATISTICAL DISCRIMINATION OF FRACTAL AND MARKOV MODELS OF SINGLE-CHANNEL GATING

STEPHEN J. KORN AND RICHARD HORN
Neurosciences Department, Roche Institute of Molecular Biology, Nutley, New Jersey 07110

ABSTRACT A statistical comparison is presented of Markov and fractal models of ion channel gating. The analysis is based on single-channel data from two types of ion channels: open times from a 90 pS Ca-activated K channel from GH_3 pituitary cells, and closed times from a nonselective channel from rabbit corneal endothelium (Liebovitch et al., 1987*a*). Maximum likelihood methods were used to fit the data. For both data sets the best Markov model had three exponential components. The best Markov model had a higher likelihood than the fractal model, and the Asymptotic Information Criterion favored the Markov model for each data set. A more detailed analysis, using the Monte Carlo methods described in Horn (1987), showed that the Markov model was not significantly better than the fractal model for the corneal endothelium channels. The inability to discriminate the models definitively in this case was shown to be due in part to the small size of the data set.

INTRODUCTION

As first suggested by the work of Hodgkin and Huxley (1952), and subsequently reformulated by Fitzhugh (1965), modeling of ion channel gating has been rooted in the concepts of classical kinetics. In accord with these concepts, channels are proposed to exist in a finite number of discrete states, with transitions between states governed by first order rate constants. The additional assumption that the rate constant is independent both of time and of the preceding history of the channel defines the model as a time-homogeneous Markov chain model.

Although Markov chain models often fit experimental data quite well (cf., Magleby and Pallotta, 1983*a*, *b*; Horn, 1984; Pallotta, 1985), the possible existence of other, more satisfactory, models remains. In fact, several conceptually different models of ion channel gating have been proposed (Rubinson, 1982; Fishman, 1985). Recently, Liebovitch et al. (1987*a*, *b*, *c*) applied Mandelbrot's (1983) fractal concepts to the gating of ion channels. In contrast to Markovian assumptions, it is assumed in Liebovitch's fractal model that the channel can exist in an infinite number of energy states, perhaps due to subtle differences in protein conformation. Consequently, transitions from one conductance state to another would be governed by a continuum of rate constants. The simplest fractal model of ion channel gating postulates that there is one nonconducting (*closed*) and one conducting (*open*) state, and that the rates for transition between these states vary as a function of time (Liebovitch et al., 1987*a*, *b*, *c*).

Here, we used statistical methods to compare Markov and fractal models of single-channel dwell time data. Two data sets were analyzed as examples: Ca-activated K channel open times, which have been extensively characterized using Markov models (e.g., see Magleby and Pallotta, 1983*a*, *b*; Pallotta, 1985; McManus and Magleby, 1988), and corneal endothelium channel closed times, which Liebovitch et al. (1987*a*, *b*) have described as fractal.

METHODS

Patch-clamp Recording of Single-Channel Currents

The gigaseal patch clamp technique (Hamill et al., 1981) was used to record single-Ca-activated K channel currents from outside-out membrane patches, excised from cultured GH_3 pituitary cells. Patch pipettes, fabricated from N51A glass, were coated internally and externally with Sigmacote (Sigma Chemical Co., St. Louis, MO) and externally with Sylgard (Dow Corning Corp., Midland, MO). The pipette solution (facing the internal membrane face) consisted of (in mM): KCl, 150; HEPES, 10; EGTA, 1.1; $CaCl_2$, 0.92; and sucrose, 15 ([Ca] = 0.5 μM, pH (adjusted with NaOH) = 7.36, osmolality = 319). The bath solution (facing the external membrane face) consisted of (in mM): NaCl, 140; KCl, 5; $MgCl_2$, 10; Hepes, 10 and glucose, 20 (pH = 7.36, osmolality = 332). Apamine (200 nM, Sigma Chemical Co.) was added to the bath solution to block a small conductance K channel. Single-channel currents (Fig. 1 *A*) were filtered at 20 KHz, recorded on FM tape at 30 inches/s (bandwidth = 16 KHz), and digitized from the tape at 80 KHz.

Dwell Time Histograms

Ca-activated K channel open times were calculated using a half-maximum threshold detection technique (Colquhoun and Sigworth, 1983). 12,148 opening events were measured from a continuous recording at a holding potential of +20 mV; the open dwell times ranged from 12.5 μs (the sample interval) to 9.8375 ms in duration. Dr. L. Liebovitch kindly provided us with 1,465 closed times measured from single rabbit corneal endothelium channels (Liebovitch et al., 1987*a*). These dwell times ranged from 1.65 ms to 1.185 s. Except as noted, dwell time histograms were plotted with time on the abscissa logarithmically transformed, and the number of events on the ordinate transformed by the power of one-half (Sigworth and Sine, 1987).

Correction for Sampling Promotion Error

Dwell times measured at a discrete sample interval are subject to a binning error known as sampling promotion error (McManus et al., 1987), which is due to the fact that dwell times are clustered at multiples of the sample interval. Two strategies are presently available to avoid the statistical bias caused by this error. The first is to correct the likelihood function for fitting the data (McManus et al., 1987). The second is to interpolate the experimental current trace in the vicinity of threshold crossings, thus avoiding the usual binning of the data at multiples of the sample interval (Colquhoun and Sigworth, 1983; Sigworth and Sine, 1987).

We have chosen another strategy, which provides an approximate correction. The probability $p(N|t)$ for an event covering N sample intervals, given a true duration t, is a triangular function between $N-1$ and $N+1$ sample intervals (Sine and Steinbach, 1986; McManus et al., 1987). If it is assumed that the true probability density of dwell time is constant over each bin (i.e., the bin width is narrow compared with the fastest decay of this density), then the conditional density $p(t|N)$ is also a triangular function given by

$$p(t|N) = \begin{cases} [(t/T) + 1 - N]/T & (N-1)T \le t < NT \\ [N + 1 - (t/T)]/T & NT \le t < (N+1)T, \\ 0 & \text{elsewhere} \end{cases}$$

where T is the sample interval (12.5 μs for our data).

Whereas the true dwell times can be of any duration, the measured dwell times fall into bins, at intervals NT (where $N = 1, 2, \ldots$), that are multiples of the same interval, T. To correct for this error, the events in each bin were probabilistically redistributed according to the above density, $p(t|N)$. This was done by calculating the probability for events in the Nth bin to be located in any interval between $(N-1)T$ and $(N+1)T$.

For dwell times between $(N-1)T$ and NT the probability of an event falling in the interval (t_1, t_2) is

$$T^{-1}[(t_2^2 - t_1^2)/2T + (1 - N)(t_2 - t_1)].$$

For dwell times between NT and $(N+1)T$ the probability of an event falling in the interval (t_1, t_2) is

$$T^{-1}[(N+1)(t_2 - t_1) - (t_2^2 - t_1^2)/2T].$$

In practice, when data are binned linearly, the correction for sampling promotion error is simple. One fourth of the data is moved out of the Nth bin; one eighth goes into the $(N-1)$th bin and one eighth goes into the $(N+1)$th bin. For log-binning, the bin limits (t_1, t_2) must be determined (see Sigworth and Sine, 1987). Then the data in the original Nth bin are redistributed, according to the above probabilities, among all log bins between $(N-1)T$ and $(N+1)T$. Note that these corrections for sampling promotion error convert the histogram bins from integers to reals. It should also be noted that this correction is only approximate, since it is assumed that bin widths are small enough that the density of dwell times is constant over each bin. Our statistical analysis used log-binned data at a density of 16 bins per decade. Decreasing the bin widths to 25 bins per decade changed the estimates of time constants by <1%, which suggests that the correction was adequate for our data.

Logarithmic Transformation of Markov and Fractal Models

For the logarithmic transformation of time, $x = \ln(t)$. The probability density function for an N-exponential Markov model of dwell time is (Sigworth and Sine, 1987):

$$g(x) = \sum_{i=1}^{N} w_i \exp[x - x_i - \exp(x - x_i)], \quad (1)$$

where w_i and x_i are the weight and logarithm of the ith time constant. One of the several advantages of this method of display is that, when using Markov models, peaks occur at the time constants for transitions between states (where $x = x_i$). As shown below, this contrasts with the results obtained for the fractal model.

The fractal model of ion channel kinetics assumes that the kinetic rate k for transition from one state to another is a function of the time scale in which it is observed. The rate may be expressed as $k = At^{1-D}$, where A is the kinetic setpoint and D is the fractal dimension (Liebovitch et al., 1987*a*, *b*, *c*). For a physically and mathematically plausible density function, $1 \le D < 2$. When $D = 1$, the rate is independent of time, and the scheme for this transition reduces to a single exponential, Markov model. For $D > 1.0$, as a channel remains in a particular state longer, the rate for leaving that state becomes smaller.

The cumulative distribution function for a channel that exhibits fractal properties is:

$$F(t) = 1 - \exp\{[-A/(2 - D)]t^{2-D}\}. \quad (2)$$

Following log transformation of time (t), the distribution function is:

$$G(x) = F[\exp(x)] = 1 - \exp\{[-A/(2 - D)][\exp(x)]^{2-D}\}. \quad (3)$$

The corresponding probability density function is:

$$g(x) = A[\exp(x)]^{2-D} \exp\{[-A/(2 - D)] \cdot [\exp(x)]^{2-D}\}. \quad (4)$$

In contrast to the density function for a Markov model (Eq. 1), this fractal density function is always unimodal, with the peak at

$$x = -ln[A/(2 - D)]/(2 - D). \quad (5)$$

Note that the histograms in Figs. 2 and 3 were plotted using $\log_{10}$(time) rather than the natural logarithm of time, and were plotted at a bin density of 10 bins per decade.

Fitting the Dwell Time Distributions

Maximum likelihood methods were used to estimate the parameters for both Markov and fractal models. For fitting, the data were log-binned at a density of 16 bins per decade, and the likelihood was calculated for the data to fall within the upper and lower limits of each bin (Sigworth and Sine, 1987). The likelihood was calculated for dwell times $\ge t_{min}$ (e.g., see Horn, 1987; Sigworth and Sine, 1987), because events shorter than t_{min} were assumed to be under-represented due to errors related to low-pass filtering (Colquhoun and Sigworth, 1983). For Ca-activated K channels, t_{min} was 37.5 μs. For the corneal endothelium channel, t_{min} was 1.65 ms. The likelihood was maximized by a variable metric algorithm kindly provided by Dr. Kenneth Lange.

Theoretical distributions were calculated for each data set by substitution of the appropriate maximum likelihood estimates into Eqs. (1) and (4). For comparison with the experimental data, these distributions were scaled using Eq. (10) in Sigworth and Sine (1987).

Simulations and Model Comparisons

Simulation of data was used in some of the statistical procedures. In each case, the inverse of the appropriate density function was determined (e.g., see Blatz and Magleby, 1986; Horn, 1987). For the fractal model, a random dwell time, t, was simulated from the equation,

$$t = [-(2 - D)ln(\text{RAN})/A]^{(2-D)^{-1}},$$

where RAN is a uniformly distributed random number between 0.0 and 1.0.

The methods of model discrimination followed the procedures in Horn

(1987). The best Markov models were determined by sequential likelihood ratio tests and the comparisons between Markov and fractal models used procedures appropriate for nonnested models.

RESULTS

Ca-activated K Channels

Ca-activated K channels (90 pS) were recorded from an outside-out patch at a holding potential of +20 mV (Fig. 1 *A*). This patch contained two channels, but under these experimental conditions, openings of both channels overlapped in fewer than 0.5% of 12,148 observed events. Likelihood estimates were obtained for five models of channel closing: four Markov chain models consisting of one, two, three, or four exponentials and a fractal model. Dwell times <37.5 μs were excluded from the analysis (see arrow in Fig. 2). The remaining data set consisted of 11,677 dwell times. Maximum log-likelihood values for each model are presented in Table I. Using a likelihood ratio test, the three-exponential Markov model was clearly superior to the one- and two-exponential Markov models. The four-exponential model was not better statistically (data not shown). Both the likelihood ratio test and the Asymptotic Information Criterion (AIC, Akaike, 1974; Horn, 1987) indicated that the three-exponential model (model M) was better than the fractal model (model F). If the log likelihood ratio (LLR) is defined as the logarithm of the ratio of the maximum likelihood of model F to that of model M, and k_i is the number of free parameters in model i, then

$$\mathrm{AIC} = \mathrm{LLR} - (k_F - k_M) = -801.36.$$

Because the AIC value is less than zero, it is concluded that the Markov model is better. The statistical significance of this value is evaluated below.

Open time histograms were constructed in two ways.

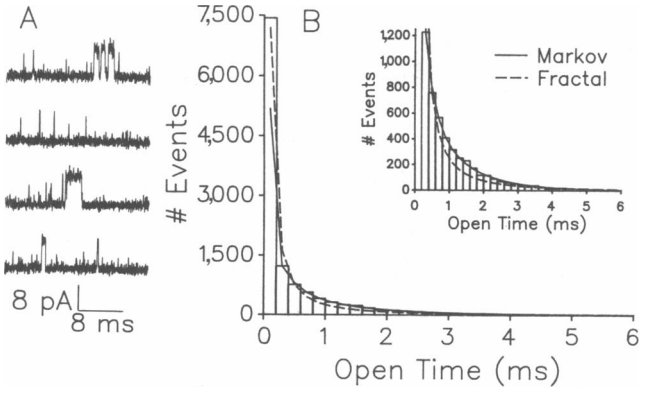

FIGURE 1 Open times for Ca-activated K channels. (*A*) Examples of 25.6 ms segments of the data recorded continuously at a holding potential of +20 mV. Openings are upward transitions. (*B*) Linear histogram of open times. Data were corrected for sampling promotion error (see Methods). The best-fit theory curves for corrected data are superimposed on the histogram. The best Markov model had three exponential components. The insert shows the data scaled for dwell times >200 μs.

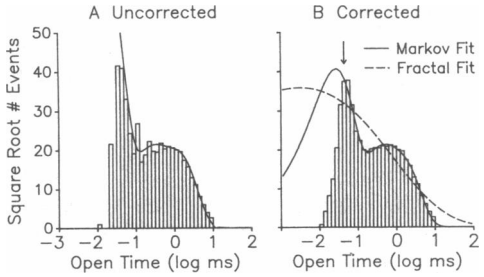

FIGURE 2 Log-binned histograms of open times for Ca-activated K channels. Same data as in Fig. 1. *A* and *B* show data uncorrected and corrected for sampling promotion error. The best Markov model for each case is superimposed. The best fractal model of the corrected data is shown (*dashed line*) in *B*. The arrow indicates the minimum duration of data used in the fit. The parameters for the models in *B* are given in Table I. The parameters for the model in *A* are: r_1, r_2, r_3 = 65.84, 5.243, 0.9369 ms^{-1}; w_1, w_2, w_3 = 0.8831, 0.0465, and 0.0704.

The standard technique, plotting the number of events per bin as a function of time, is shown in Fig. 1 *B*. These data were corrected for sampling promotion error (see Methods). In Fig. 2 the data were binned according to the method of Sigworth and Sine (1987); the square root of the number of events is plotted as a function of the logarithm of time. As described by Sigworth and Sine, log-binned histograms provide information graphically that is not obvious from linear histograms. Markov models predict peaks in a log-binned histogram, each of which corre-

TABLE I
MAXIMUM LOG LIKELIHOODS AND ESTIMATED KINETIC PARAMETERS FOR MARKOV AND FRACTAL MODELS

Ca-activated *K* channel		Corneal endothelium channel	
Maximum log likelihoods and log likelihood ratio (LLR) from 3 Markov models and fractal model.			
model	max. log likelihood	model	max. log likelihood
1 state	−41376.49	1 state	−5849.503
2 state	−36228.23	2 state	−5338.293
3 state	−36123.12	3 state	−5252.357
fractal	−36927.48	fractal	−5256.369
LLR ($LL_F - LL_M$) = −804.36		LLR ($LL_F - LL_M$) = −4.012	
Best fit kinetic parameters, 3 state Markov model.			
r_1 = 37.85 ± 1.06		r_1 = 0.398 ± 0.050	
r_2 = 3.440 ± 0.409		r_2 = 0.037 ± 0.003	
r_3 = 0.888 ± 0.031		r_3 = 0.006 ± 0.001	
w_1 = 0.73 ± 0.01		w_1 = 0.46 ± 0.02	
w_2 = 0.11 ± 0.01		w_2 = 0.43 ± 0.02	
w_3 = 0.16 ± 0.01		w_3 = 0.11 ± 0.02	
Best fit kinetic parameters, fractal model.			
A = 4.56 ± 0.08		A = 2.50 ± 0.14	
D = 1.77 ± 0.01		D = 1.63 ± 0.01	

r_1, r_2, r_3 are rate constants (units of ms^{-1}), and w_1, w_2, and w_3 are associated weighting factors in the density function in Eq. 1 ($r_i = 1/\exp[x_i]$). A is the kinetic setpoint (units of $Hz^{(2-D)}$) and D is the fractal dimension in the density function in Eq. 4.

sponds to the logarithm of a time constant (Sigworth and Sine, 1987). In contrast, the fractal model predicts only a single peak (Eq. 5 above; Horn and Korn, 1988). The presence of two prominent peaks in Fig. 2 is itself sufficient to exclude the fractal model from consideration (Horn and Korn, 1988). Fig. 2 also shows the effect of correcting the data for sampling promotion error (see Methods). Fig. 2 *A* shows uncorrected and Fig. 2 *B* shows corrected data.

Theoretical curves, calculated using the three-exponential Markov model and the fractal model, are superimposed on the histograms in Figs. 1 and 2. The parameters used for each curve are listed in Table I. As expected from the LLR, the data are fit better by the Markov model. Note that only two peaks are evident in the plots of Fig. 2, whereas the Markov model predicts three peaks corresponding to the three exponential components. This is due to the fact that the two slower time constants are so close that they form one broad peak.

Corneal Endothelium Channels

Closed time histograms, derived from single-channel data collected by Liebovitch et al. (1987*a*) from corneal endothelium, are presented in Fig. 3. The data set consists of 1,465 dwell times. Likelihoods for all five models were evaluated for dwell times ≥1.65 ms, the shortest dwell time in this data set. The parameter values which gave the best fits and the likelihoods are presented in Table I. The best Markov model, by likelihood ratio test, had three exponential components. The likelihood was not improved significantly for a model with four components. Theoretical curves were calculated using the likelihood estimates (Table I) for the three-exponential Markov model (Fig. 3 *A*) and the fractal method (Fig. 3 *B*, *solid line*). For comparison, the theoretical curve for the fractal model using parameters obtained by Liebovitch et al. (1987*a*) is shown (Fig. 3 *B*, *dashed line*). No correction was made for sampling promotion error in our analysis of these data, because the dwell times were measured manually (L. Liebovitch, personal communication), and therefore do not conform with the probabilistic description in McManus et al. (1987). When we used our correction on these data, the LLR decreased in favor of the Markov model (data not shown). The AIC criterion, which chooses one model over another, suggested that the Markov model was marginally superior (AIC = −1.012).

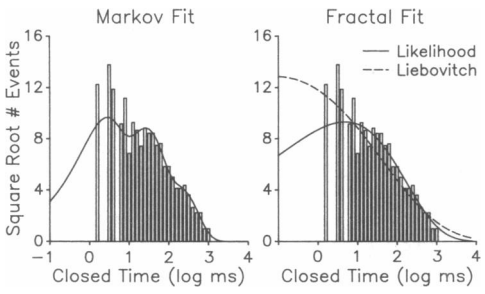

FIGURE 3 Log-binned histograms of closed times for corneal endothelium channels. The data were not corrected for sampling promotion error. *A* shows the best Markov model and *B* shows the best fractal model (*smooth line*). The dashed line in *B* is the fractal model using the parameters estimated by Liebovitch et al. (1987*a*) for the same data (A = 1.49 $Hz^{0.21}$ and D = 1.79). Other model parameters are given in Table I.

Non-nested Model Comparisons

Although the data shown for Ca-activated K channels (Figs. 1 and 2) clearly favored a three-exponential Markov model over the fractal alternative, the situation was not so obvious for the data in Fig. 3. First, the presence of discrete peaks is not convincing in Fig. 3. Furthermore, the AIC value for these data is close to zero, which suggests that the two models may be statistically indistinguishable for this data set. This ambiguity can be addressed by more elaborate statistical procedures which use Monte Carlo methods (Horn, 1987). We will demonstrate these methods first with the data obtained from Ca-activated K channels.

Two procedures, described in detail in Horn (1987), were used to assign a significance level to the comparison of the two models. In the first procedure, 1,000 data sets were simulated under the assumption that one or the other model was correct. These data sets were simulated using the maximum likelihood estimates calculated from the original data, either for the three-exponential Markov model or for the fractal model. The size of each data set was the same as that of the original one, 11,677 dwell times >37.5 μs. A value for LLR ($LL_F - LL_M$) was then obtained for each data set using the best fit from each model. The distribution of 1,000 LLRs obtained from each simulation is shown in the upper part of Fig. 4. The distribution on the left represents LLRs obtained when

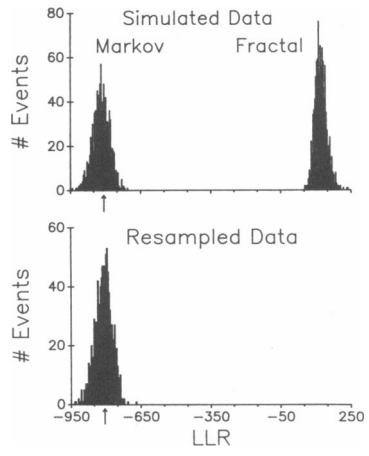

FIGURE 4 Comparison of best Markov and fractal models for open times of Ca-activated K channels. The upper plot shows the empirical distribution of LLRs for the fractal versus Markov models with data simulated by the Markov model (*left*) or the fractal model (*right*). The original LLR (*arrow*) is consistent with the Markov model but not the fractal model. The lower plot is the distribution of LLRs for resampled data. The distribution is much less than zero, in support of the Markov model.

data were simulated using the Markov model; the distribution on the right was obtained when the fractal model was used to simulate the data. The arrow below the histogram designates the original LLR, obtained from the best fit of the real data. The original LLR is a possible member of the population of LLRs simulated under the Markov model, but is distinct from the fractal population. This plot shows that, for the parameters given in Table I, it is possible to discriminate accurately between the fractal and Markov models for every data set.

The second procedure for statistically comparing the models involved estimating the variability of LLR of the original data. To do this, 1,000 data sets containing 11,677 intervals were generated by randomly resampling the original 11,677 intervals with replacement. Maximum likelihood estimates were calculated for each resampled data set using the Markov and fractal model. The distribution of LLRs ($LL_F - LL_M$) for each resampled data set is plotted in the lower panel of Fig. 4. The LLR for the original data set is shown by the arrow below the distribution. Ignoring parsimony, if the value of LLR is <0, the data are consistent with the Markov model. If the LLR is >0, the data are consistent with the fractal model (a value of 0 suggests that the models are not statistically different, in terms of likelihood). The distribution of LLRs for the resampled data in Fig. 4 is entirely below zero, i.e., the likelihood was greater for the Markov model in each of the 1,000 data sets. This result again supports the conclusion that the Markov model is superior to the fractal model for open times of Ca-activated K channels. A consideration of parsimony would change the critical value from zero to −3, the difference in the number of free parameters between the two models (Horn, 1987). This consideration has no effect on the choice of the Markov over the fractal model.

These methods become more important for analysis of the closed times of corneal endothelium channels. In this case both the AIC value and the plots of Fig. 3 suggest that the two types of model are more difficult to discriminate. Fig. 5 shows the analysis of these models using simulation (*upper panel*) and resampling (*lower panel*). These distributions of LLRs show several characteristics that differ from those of Fig. 4. First, the distributions of LLRs for simulated Markov and fractal models overlap, showing that simulated data sets from the two types of model are more similar in terms of likelihood. Second, the original LLR (−4.012) falls in the tails of the simulated distributions of both models. Based on the mean and standard deviation of each of these two approximately Gaussian distributions (see legend of Fig. 5), the original LLR has a probability $P = 0.012$ of being a member of the Markov distribution and $P = 0.025$ for the fractal distribution. Based on the rank order of these distributions, the original LLR has a probability of 0.006 of being a member of the Markov distribution and 0.012 for the fractal distribution. Using typical significance levels for hypothesis tests (e.g., $\alpha = 0.01$–0.05), these probabilities are marginal in terms of rejecting the appropriate null hypotheses. Third, the distribution of LLRs of resampled data includes both zero ($P = 0.110$) and the AIC value (−1.012, $P = 0.158$), indicating that the two models are indistinguishable (Horn, 1987). In total, the analysis shown in Fig. 5 suggests that the data for corneal endothelium channels cannot lead to a clear choice between Markov and fractal models. We discuss below some of the possible problems in making a discrimination for these data.

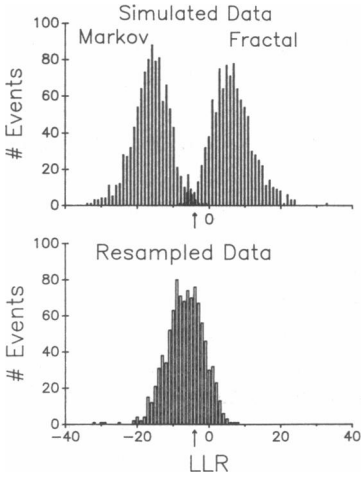

FIGURE 5 Comparison of best Markov and fractal models for closed times of corneal endothelium channels. The upper plot shows the empirical distribution of LLRs for the fractal versus Markov models with data simulated by the Markov model (*left*) or the fractal model (*right*). The original LLR (*arrow*) barely falls within the tails of both distributions. The Markov distribution (*left*) has a mean of −15.74 and a standard deviation of 5.16. The fractal distribution (*right*) has a mean of 7.02 and a standard deviation of 5.63. The lower plot is the distribution of LLRs for resampled data. The distribution includes both zero and the AIC value of −1.012, having a mean of −6.20 and a standard deviation of 5.16.

DISCUSSION

Our goal here was to present a rigorous method for choosing between Markov and fractal models of ion channel gating. These two classes of models represent markedly different views of channel gating, and would require different types of hypotheses regarding gating mechanisms. Markov chain models assume that channels exist in a finite number of significant energy states, whereas Liebovitch's fractal model assumes that channels exist in an infinite number of significant energy states. In practical terms, the primary difference between the two models is in the time-dependence of the transition rates; the fractal model assumes that the transition rate from one state to another is a function of time (Liebovitch et al., 1987*a*, *b*, *c*), whereas Markov models are time-homogeneous (Colquhoun and Hawkes, 1981, 1983; Horn, 1984). The statistical methods for comparison of these models are necessarily complicated, because the models are non-

nested (one model cannot be described as a smoothly parametrized subhypothesis of the other, Horn, 1987).

We chose for our analysis two data sets of single-channel dwell times, one that has been extensively described using Markov chain models and one that was previously described as fractal. Analysis of >11,000 Ca-activated K channel open times strongly favored a three-exponential Markov model over the fractal alternative. A similar analysis of 1,465 closed times from corneal endothelium channels demonstrated, however, that for this data set, the two models could not be discriminated.

The failure to discriminate between the three-exponential Markov and the fractal model for corneal endothelium channels was due to an insufficient amount of data. The density functions for these models are mathematically distinct (except that both models can be reduced to a single-exponential density for specific parameter values). The available data set had only 1,465 dwell times. If it had, for example, as many dwell times (11,677) as we used for analysis of Ca-activated K channels, the discrimination would have been possible. This is shown in Fig. 6. Data sets of 11,677 dwell times ≥1.65 ms were simulated under each model, using the parameter estimates in Table I. The resultant distributions of LLRs are plotted in Fig. 6. These distributions are well separated, and neither one includes zero. This means that, for these parameters and a data set of this size, the models are always distinguishable. This fact is especially apparent when considering the data simulated under a fractal model. Every LLR was much greater than zero despite the three additional free parameters of the Markov model, which indicates that every 11,677 event data set simulated by the fractal model was unambiguously fractal.

Another insufficiency of the available data set for this type of channel was the frequency limitation; data were limited to dwell times ≥1.65 ms. It is probable that a greater resolution of dwell times would help the discrimination, especially since most of the data in the fractal model occurs at much faster dwell times (Horn and Korn, 1988).

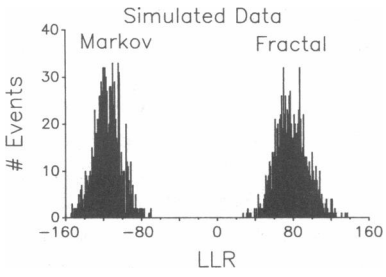

FIGURE 6 Histograms of LLRs from data simulated under the Markov (*left*) or fractal (*right*) model using parameters for the corneal endothelium channel but a larger sample size for each data set (see text). The empirical distributions are well-separated and distinct from zero, showing that the models are distinguishable for data sets of this size (i.e., 11,677 dwell times).

We have used maximum likelihood methods to fit all of the data. This contrasts with the methods used by Liebovitch et al. (1987*a*, *b*, *c*). Our estimates of fractal parameters for their single-channel data differ from their estimates. Our maximum likelihood estimates of A and D are 2.50 ± 0.14 $Hz^{0.37}$ and 1.63 ± 0.01. Their estimates of A and D were 1.49 $Hz^{0.21}$ and 1.79 (Liebovitch et al., 1987*a*). Fig. 3 *B* has plots of the density function using both sets of parameters. Although both curves seem to fit the data qualitatively, the maximum likelihood estimates, by definition, yield a density function with a greater likelihood. The justifications for use of maximum likelihood estimates are well known (e.g., see Rao, 1973). Specifically, maximum likelihood estimates are unbiased and have minimum variance among all unbiased estimates. Furthermore, maximum likelihood estimation extracts all of the relevant information that the data can provide about the parameters being estimated (e.g., see Ferguson, 1967, chapter 3). Finally, the likelihoods themselves may be used for likelihood ratio tests and comparisons of non-nested models (Horn, 1987).

Our analysis does not address the usefulness of fractal models for modeling the behavior of these channels under other conditions or for modeling channel behavior in general. However, our results are in agreement with a similar analysis of dwell times from four different types of ion channels (McManus and Magleby, 1988; McManus et al., 1988). Furthermore, we know of no example where a fractal model is clearly superior to a Markovian alternative. In fact, the literature is already replete with dwell time histograms that could not be fit with a fractal model of the form proposed by Liebovitch et al. (1987*a*, *b*, *c*), because the multiple components are readily identified visually (e.g., see Camardo and Siegelbaum, 1983; Magleby and Pallotta, 1983*a*, *b*; Sigworth, 1983; Blatz and Magleby, 1986; Hestrin et al., 1987; Sigworth and Sine, 1987; Horn and Korn, 1988; Papke et al., 1988).

We thank Dr. Larry Liebovitch for providing us with his data. Drs. Karl Magleby and Larry Liebovitch treated us to colorful dialogues and insightful comments on the manuscript.

Supported in part by National Institutes of Health Postdoctoral Fellowship NS08117 to Dr. Korn.

Received for publication 14 March 1988 and in final form 5 July 1988.

REFERENCES

Akaike, H. 1974. A new look at the statistical model identification. *IEEE (Inst. Electr. Electron. Eng.) Trans. Biomed. Eng.* AC-19:716–723.

Blatz, A. L., and K. L. Magleby. 1986. Quantitative description of three modes of activity of fast chloride channels from rat skeletal muscle. *J. Physiol. (Lond.).* 378:141–174.

Colquhoun, D., and A. G. Hawkes. 1981. On the stochastic properties of single ion channels. *Proc. R. Soc. Lond. B Biol. Sci.* 211:205–235.

Colquhoun, D., and A. G. Hawkes. 1983. The principles of stochastic interpretation of ion-channel mechanisms. *In* Single Channel Recording, B. Sakmann and E. Neher, editors. Plenum Publishing Corp., New York. 135–175.

Colquhoun, D., and F. Sigworth. 1983. Fitting and statistical analysis of single-channel records. *In* Single Channel Recording. B. Sakmann and E. Neher, editors. Plenum Publishing Corp., New York. 191–264.

Ferguson, T. S. 1967. Mathematical Statistics. A Decision Theoretic Approach. Academic Press, Inc., New York. 98–142.

Fishman, H. M. 1985. Relaxations, fluctuations and ion transfer across membranes. *Prog. Biophys. Mol. Biol.* 46:127–162.

Fitzhugh, R. 1965. A kinetic model of the conductance changes in nerve membrane. *J. Cell. Comp. Physiol.* 66:111–118.

Hestrin, S., J. I. Korenbrot, and A. V. Maricq. 1987. Kinetics of activation of acetylcholine receptors in a mouse cell line under a range of acetylcholine concentrations. *Biophys. J.* 51:449–455.

Hamill, O. P., A. Marty, E. Neher, B. Sakmann, and F. G. Sigworth. 1981. Improved patch-clamp techniques for high resolution current recording from cells and cell-free membrane patches. *Pfluegers Arch. Eur. J. Physiol.* 391:85–100.

Hille, B. 1984. Ionic Channels of Excitable Membranes. Sinauer Associates.

Hodgkin, A. L., and A. F. Huxley. 1952. A quantitative description of membrane current and its application to conduction and excitation in nerve. *J. Physiol. (Lond.).* 117:500–544.

Horn, R. 1984. Gating of channels in nerve and muscle: a stochastic approach. *In* Ion Channels: Molecular and Physiological Aspects. W. D. Stein, editor. Academic Press, Inc., New York. 53–97.

Horn, R. 1987. Statistical methods for model discrimination. Applications to gating kinetics and permeation of the acetylcholine receptor channel. *Biophys. J.* 51:255–263.

Horn, R., and S. J. Korn. 1988. Graphical discrimination of Markov and fractal models of single channel gating. *Topics in Theoretical Biology.* In press.

Liebovitch, L. S., J. Fischbarg, J. P. Koniarek, I. Todorova, and M. Wang. 1987*a*. Fractal model of ion channel kinetics. *Biochim. Biophys. Acta.* 896:173–180.

Liebovitch, L. S., J. Fischbarg, and J. P. Koniarek. 1987*b*. Ion channel kinetics: a model based on fractal scaling rather than multistate Markov processes. *Math. Biosci.* 84:37–68.

Liebovitch, L. S., and J. M. Sullivan. 1987*c*. Fractal analysis of a voltage-dependent potassium channel from cultured mouse hippocampal neurons. *Biophys. J.* 52:979–988.

Magleby, K. L., and B. S. Pallotta. 1983*a*. Calcium dependence of open and shut interval distributions from calcium-activated potassium channels in cultured rat muscle. *J. Physiol. (Lond.).* 344:585–604.

Magleby, K. L., and B. S. Pallotta. 1983*b*. Burst kinetics of single calcium-activated potassium channels in cultured rat muscle. *J. Physiol. (Lond.).* 344:605–623.

Mandelbrot, B. B. 1983. The Fractal Geometry of Nature. W. H. Freeman & Co. Publishers, San Francisco.

McManus, O. B., and K. L. Magleby. 1988. Kinetic states and modes of single large conductance calcium-activated potassium channels in rat skeletal muscle. *J. Physiol. (Lond.).* 402:79–120.

McManus, O. B., A. L. Blatz, and K. L. Magleby. 1987. Sampling, log binning, fitting, and plotting durations of open and shut intervals from single channels and the effects of noise. *Pfluegers Arch. Eur. J. Physiol.* 410:530–553.

McManus, O. B., D. S. Weiss, C. E. Spivak, A. L. Blatz, and K. L. Magleby. 1988. Fractal models are inadequate for the kinetics of four different ion channels. *Biophys. J.* 54:859–870.

Miller, C. 1986. Ion Channel Reconstitution. Plenum Publishing Corp., New York.

Pallotta, B. S. 1985. Calcium-activated potassium channels in rat muscle inactivate from a short-duration open state. *J. Physiol. (Lond.).* 363:501–516.

Papke, R. L., G. Millhauser, Z. Lieberman, and R. E. Oswald. 1988. Relationships of agonist properties to the single channel kinetics of nicotinic acetylcholine receptors. *Biophys. J.* 53:1–10.

Rao, C. R. 1973. Linear Statistical Inference and Its Applications. 2nd ed. John Wiley & Sons, Inc., New York.

Rubinson, K. A. 1982. The sodium currents of nerve under voltage clamp as heterogeneous kinetics. *Biophys. Chem.* 15:245–262.

Sakmann, B., and E. Neher. 1983. Single Channel Recording. Plenum Publishing Corp., New York.

Sine, S. M. and J. H. Steinbach. 1986. Activation of acetylcholine receptors on clonal mammalian BC3H-1 cells by low concentrations of agonist. *J. Physiol. (Lond.).* 373:129–162.

Sigworth, F. J. 1983. An example of analysis. *In* Single Channel Recording. B. Sakmann and E. Neher, editors. Plenum Publishing Corp., New York. 301–321.

Sigworth, F. J., and S. M. Sine. 1987. Data transformations for improved display and fitting of single-channel dwell time histograms. *Biophys. J.* 52:1047–1054.